ACTA ABP BIOCHIMICA POLONICA

Vol. 69, No 2/2022
399–407
https://doi.org/10.18388/abp.2020_5851

Regular paper

Proteomics analysis of lipid droplets in mouse neuroblastoma cells

Weiyi Wang[1]✉, Jiahao Guan[2], Yu Zong[2], Qiuxian Zhang[2], Wei Zhang[3] and Hecheng Wang[2]✉

[1]Department of Cardiovascular Diseases, Civil Aviation General Hospital, Peking University, Beijing, China; [2]School of Life and Pharmaceutical Sciences, Dalian University of Technology, Panjin, China; [3]School of basic medical sciences, Xinxiang medical university, Xinxiang, China

Lipid droplets (LDs) are intracellular droplets containing phospholipids and neutral lipids. It is well known that LDs are organelles with a rich proteome. In the nervous system, these droplets may play an important role in maintaining the normal physiological function of nerve cells. Moreover, LDs may relate to the neurodegenerative disorders, such as Alzheimer's disease (AD). However, more information is still needed about the function of LDs. In the study presented here, we identified the protein composition of mouse neuroblastoma (N_2a) cell LDs using immunodetection and high-performance liquid chromatography (HPLC) coupled with mass spectrometry (MS). Seventy three LDs proteins were identified. Gene ontology (GO) and Kyoto Encyclopedia of Genes and Genomes (KEGG) pathway enrichment analyses were performed to investigate the potential functions of these proteins. Subsequently, the relationships among the proteins were analyzed by constructing a protein-protein interaction (PPI) network. N_2a cell LDs contain multiple Rab GTPases, chaperones, and proteins involved in ubiquitination and transport. Some of these proteins were known to modulate LD formation and were related to the function of nerve cells. This work presents the proteome of N_2a cell LDs and will help to identify the role of LDs in the nervous system.

Keywords: lipid droplets, proteomics analysis, mouse neuroblastoma cells, bioinformatics, neurodegenerative diseases

Received: 20 August, 2021; revised: 12 October, 2021; accepted: 12 October, 2021; available on-line: 25 May, 2022

✉e-mail: xc_wangwy@163.com (WW); wanghc@dlut.edu.cn (HW)
Funding: The following grants supported this research: the Fundamental Research Funds for Civil Aviation General Hospital (No.201932), and Liaoning Provincial Natural Science Foundation Guidance Project (ZX20190531).

Abbreviations: LDs, lipid droplets; N_2a cells, mouse neuroblastoma cells; HPLC, high-performance liquid chromatography; GO, Gene ontology; KEGG, Kyoto Encyclopedia of Genes and Genomes; CNS, the central nervous system; PPI, protein-protein interaction; PBS, phosphate-buffered saline; TLC, thin-layer chromatography; PNS, post-nuclear supernatant; SDS-PAGE, sodium dodecyl sulfate-polyacrylamide gel electrophoresis; BCA, bicinchoninic acid; BP, biological process; CC, cellular component; MF, molecular function; MS, mass spectrometry

INTRODUCTION

Lipid droplets (LDs) are intracellular organelles that mainly function in fat storage. They can be found in almost all organisms, from bacteria to mammals (Zhang & Liu, 2017). In particular, lipids account for almost half of the total dry weight of the brain. There are three major categories of brain lipids: cholesterol, sphingolipids, and glycerophospholipids (Fuller & Futerman, 2018). In addition, LDs are oil-in-water emulsion droplets containing neutral lipids covered by a phospholipid monolayer, with many proteins embedded on their surface (Kory *et al.*, 2016). The proteins in LDs are bioactive, controlling lipid storage, hydrolysis, and LD-related cellular functions (Murphy, 2012).

LDs may play a central role in lipid metabolism, providing precursors for membrane lipids and storing energy (Welte, 2015). LDs are also involved in intracellular processes of protein storage, signal transduction, and membrane trafficking. However, the mechanisms underlying contribution of LDs to the complex lipid metabolism of the nervous system have been poorly explored. A study showed that LDs in the nervous system may be involved in neuronal development and cell signaling, and thus might be related to neurodegenerative diseases (Liu *et al.*, 2015), such as Alzheimer's Disease (AD), which is an age-related disorder. However, further studies are needed to elucidate the function of LDs in the nervous system.

The purpose of this study is to clarify the functions of LD proteins using a cell model. Mouse neuroblastoma (N_2a) cells constitute a mouse neural crest-derived cell line; these cells originate from the neurons in the central nervous system (CNS) of mice (Wichmann *et al.*, 2015). They can differentiate into neuron-like cells and connect with other cells via cell links (Westergard *et al.*, 2016). Therefore, N_2a cells have been widely used in the field of neuroscience to study neuronal differentiation, axonal growth, and signaling pathways; moreover, they can be used as pathological models to study neurodegenerative diseases, inflammation, and stress (Amazzal *et al.*, 2007, Sachana *et al.*, 2003, Tremblay *et al.*, 2010). This proteomics study of LDs in N_2a cells will help elucidate the functions of LDs in the nervous system.

In view of previous research, we identified the protein composition in the LDs of mouse neuroblastoma cells using mass spectrometry (MS) and immunodetection. Then, we drafted the possible pathways of these proteins and analyzed their relationship by constructing a protein-protein interaction (PPI) network.

MATERIALS AND METHODS

Cell culture

N_2a cells which were purchased from Xiehe cell bank (Beijing, China), were cultured in Dulbecco's modified Eagle's medium (Hyclone, Utah, USA) supplemented with 10% fetal bovine serum, 100 U/mL penicillin (Sigma-Aldrich, St Louis, MO, USA), and 100 μg/mL streptomycin (Sigma-Aldrich, St Louis, MO, USA), incubated

at 37°C in an atmosphere of 5% CO_2. The cells were passaged at a ratio of 1:3 when grown to 80–90% confluence.

LD staining and thin-layer chromatography

The LDs in N_2a cells were stained with Nile Red. The N_2a cells were washed with phosphate-buffered saline (PBS) three times, and then stained with Nile Red and Hoechst 33258 for 10 min in the dark. The cells were washed with PBS three times and visualized using fluorescence microscopy (Leica, Oskar-Barnack-Strasse, Germany) at different excitation wavelengths: 352 nm and 488 nm, respectively. The total lipid contents of the LDs in N_2a cells were extracted using a method described in a previous study (Wang *et al.*, 2015). Briefly, the organic phase was collected and dried under nitrogen gas. For thin-layer chromatography (TLC) analysis, the extracts were dissolved in chloroform and loaded onto silica gel plates. The lipids were separated on plates and visualized using the iodine vapor method.

Purification of the LDs from N_2a cells

LDs were purified according to the protocol described in our previous work (Wang *et al.*, 2015, Li *et al.*, 2016, Yu *et al.*, 2015), with minor modifications. In brief, manipulations were performed at 4°C. N_2a cells were collected and homogenized using a Dounce glass homogenizer, containing 10 mL of buffer A (250 mM sucrose, 0.2 mM phenylmethylsulphonyl fluoride, 25 mM tricine, pH 7.6), with 20 strokes with a loose-fitting pestle and 40 strokes with a tight-fitting pestle. The homogenate was then disrupted in a nitrogen bomb chamber and cleaned by centrifugation at 3000×*g* using a centrifuge (Thermo Fisher Scientific, Waltham, MA, USA). The middle clear post-nuclear supernatant (PNS) at the bottom was transferred to a new tube, to be used as the cytosol (Cyto) fraction, and the pellet was collected, to be used as the total membrane (TM) fraction. The LDs were then washed three times with 200 μL of Buffer A each time. Then, they were mixed with 300 μL of acetone and 1 mL of chloroform and mixed thoroughly by vortexing. Next, the LD proteins were pelleted by centrifugation at 20,000 *g* for 10 min. The LD proteins were either subjected to proteomic analysis or dissolved in 2× sodium dodecyl sulfate (SDS)-sample buffer, and denatured at 95°C for 5 min for further analyses, such as protein profiling and western blotting. Further, for the purpose of analysis, the LD protein fractions were loaded into new tubes and mixed with Buffer B (20 mM 4-(2-hydroxyethyl)-1-piperazineethanesulfonic acid [HEPES], pH 7.4, 100 mM KCl and 2 mM $MgCl_2$) and then transferred into new tubes. The LDs were collected after centrifugation at 38000×*g* for 1 h at 4°C and washed with PBS.

Protein in-gel digestion and mass spectrometry analysis

The LD proteins were analyzed by sodium dodecyl sulfate-polyacrylamide gel electrophoresis (SDS-PAGE) and mass spectrometry after purification of the LDs from N_2a cells, according to previous studies (Wang *et al.*, 2015, Li *et al.*, 2016). Proteins in the LDs were precipitated with 100% acetone, and then separated by 10% SDS-PAGE, followed by silver staining. In brief, the fixation solution was added for 30 minutes to fix the gel; the latter was then treated with a protein treatment solution for 30 minutes and rinsed with PBS for 5 minutes and 0.5% potassium dichromate for 5 minutes. Afterward, the gel was washed with water for 5 minutes, equilibrated with 0.1% silver nitrate for 30 minutes, washed again with water for 1 minute, and incubated at pH 12 with the complex formation solution. Finally, 1% acetic acid was added to stop the complex formation. The full lane of the gel was cut into several slices according to the molecular weights of the proteins. For in-gel digestion, the gel slices were incubated with trypsin after being cut, washed, and dried; then, the extraction was vacuum-dried and dissolved. Finally, the peptides were purified and analyzed by HPLC coupled with a linear ion-trap mass spectrometer (Thermo Fisher Scientific, Waltham, MA, USA).

Protein preparation and immunoblotting

Proteins in the LDs were precipitated with 100% acetone. The protein contents were determined using the bicinchoninic acid (BCA) kit (Thermo Fisher Scientific, Waltham, MA, USA). Equal amounts (60 μg) of the proteins were loaded and separated by 10% SDS-PAGE, after which they were transferred to 0.45-μm polyvinylidene difluoride (PVDF) membranes. The membranes were then subjected to immunoblotting analysis using primary antibodies at 4°C overnight. Primary antibodies for HSL, Lamp-1, GAPDH and BIP (GRP) were purchased from Sigma-Aldrich (St Louis, MO, USA). Primary antibodies for Perilipin-1, ADRP, TIP147, CGI-58, HSD3B1, HSD17B, Tim23 were purchased from abcam (Cambridge, MA, USA). Primary antibodies for ATGL were purchased from CST (Cambridge, MA, USA). Then, the membranes were incubated with horseradish peroxidase-conjugated IgG (Sigma-Aldrich, St Louis, MO, USA). Finally, the blots were visualized using chemiluminescence detection reagents (Applygen Technologies, Beijing, China) and the FluorChem System (Protein simple, Santa Clara, California, USA).

GO and KEGG pathway enrichment analyses

Gene Ontology (GO) and Kyoto Encyclopedia of Genes and Genomes (KEGG) pathway analyses were performed to investigate the potential functions of the LD proteins. GO analysis assesses three indicators: biological process (BP), cellular component (CC), and molecular function (MF) (Ashburner *et al.*, 2000, The Gene Ontology, 2019). The analysis was performed using the Cytoscape 3.7.1 (Shannon *et al.*, 2003) plug-in ClueGO 2.5.5 (Bindea *et al.*, 2009). The analysis yielded functionally grouped networks with kappa statistics and reflected the relationships between the terms based on the similarity of their associated genes. The *P*-value was used to denote the significance of the GO terms and the enriched KEGG pathways ($P<0.05$); the *P*-values were corrected using the Benjamini–Hochberg method. Terms, represented as nodes in a grouped network, were connected based on their kappa scores (≥0.4).

PPI network construction and module analysis

The interactive relationships among proteins were analyzed by constructing a PPI network. The online database STRING (Search Tool for the Retrieval of Interacting Genes/Proteins, version 11.0, https://string-db.org/) was used to collect the interaction information for all proteins and to construct the PPI network of protein pairs with a combined score of ≥0.4 (medium confidence) (Szklarczyk *et al.*, 2019). The network was saved as a .tsv file before being imported into Cytoscape for

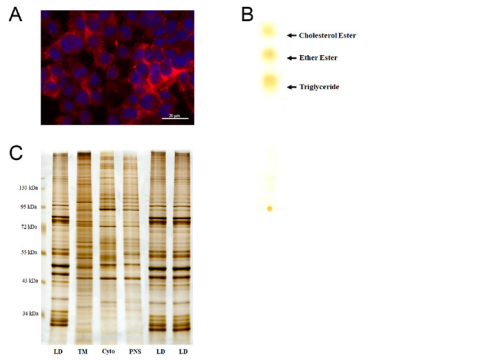

Figure 1. Lipid staining and lipid and protein patterns of LDs in N_2a cells.
(A) Lipid droplets (LDs) were stained with Nile Red, and the nuclei were stained with Hoechst 33258. The scale bar represents 20 µm. **(B)** Thin-layer chromatography analysis of LDs in N_2a cells. **(C)** Silver-stained SDS-PAGE gels of extracts of proteins in different locations in N_2a cells. LD indicates the proteins on the surface of the LDs. TM are the proteins of the total membrane. PNS depicts the proteins of the post-nuclear supernatants. Cyto represents the proteins of the cytosol.

visualization. Finally, the Cytoscape plugin MCODE 1.5.1 (Bader & Hogue, 2003) was employed to find clusters of the PPI network, with the following parameters: Degree Cutoff=4, Node Score Cutoff=0.4, K-Core=0.4, and Max. Depth=100.

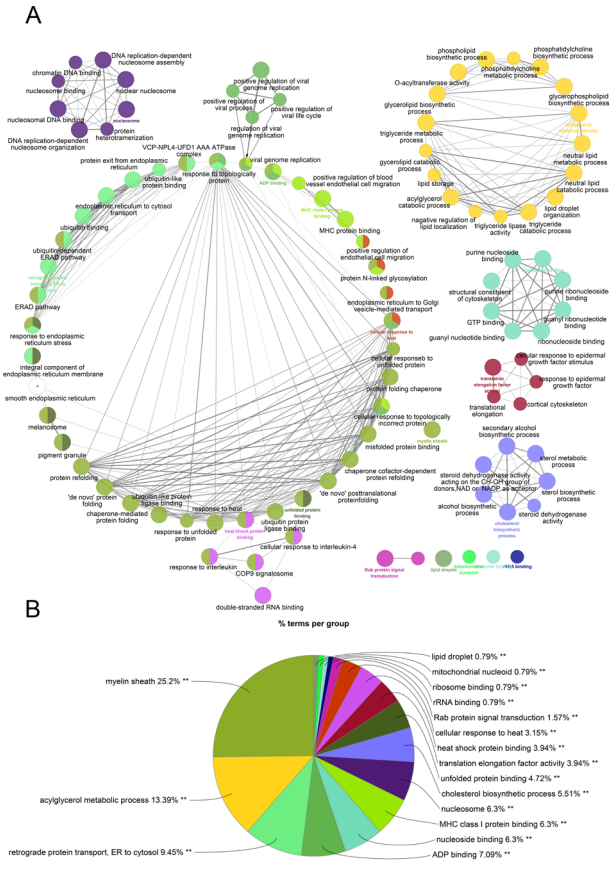

Figure 2. GO pathway enrichment analyses of all proteins.
(A) Enrichment networks resulting from the GO pathway enrichment analyses. Terms representing nodes were colored by functional groups. The size of the nodes was proportional to the enrichment *P*-value significance. Nodes were linked based on their kappa score level (≥0.4). **(B)** Pie charts of GO pathway analyses. The proportion of each group is calculated based on the number of terms included in the group. GO, gene ontology.

RESULTS

Staining LDs in N_2a cells with Nile Red

To identify the LDs, the N_2a cell cultures were stained with Nile Red. As shown in Fig. 1A, there were many LDs in the cytoplasm surrounding the cell nucleus.

Lipid and protein patterns in the N_2a cells

The TLC analysis revealed that N_2a cell LDs consisted of cholesteryl esters, triacylglycerols, and ether lipids (Fig. 1B). To identify the proteins in the N_2a cell LDs, the proteins were purified, separated by SDS-PAGE, and stained using silver nitrate. As shown in Fig. 1C, proteins in different LD preparations showed a highly consistent band pattern, indicating reliability of the LD purification.

Properties of proteins within the N_2a cell LDs

Through HPLC–MS (mass spectrometry) analysis and database searches, 73 differentially expressed proteins were identified (Table 1). The proteins were classified into seven groups based on their location and known or putative functional annotation, according to previous

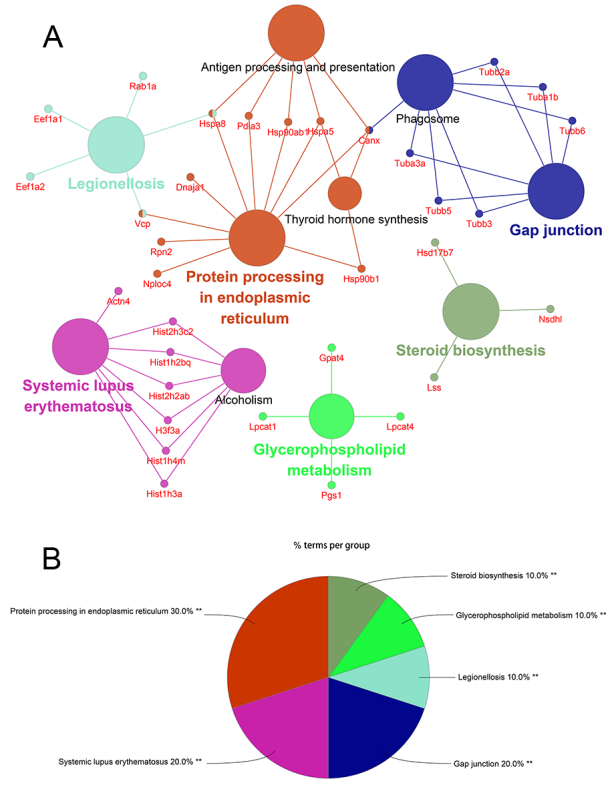

Figure 3. KEGG pathway enrichment analyses of all proteins.
(A) Enrichment networks resulting from the KEGG pathway enrichment analyses. Terms representing nodes were colored by functional groups. The size of the nodes was proportional to the enrichment *P*-value significance. Nodes were linked based on their kappa score level (≥0.4). **(B)** Pie charts of KEGG pathway analyses. The proportion of each group is calculated based on the number of terms included in the group. KEGG, Kyoto Encyclopedia of Genes and Genomes.

Table 1. 73 proteins were identified in LDs of N2a cell.

Gene symbol	GI	Description
Lipid Metabolism		
Acsl4	75992925	long-chain-fatty-acid – CoA ligase 4 isoform 2
Acsl3	209977074	long-chain-fatty-acid – CoA ligase 3 isoform a
Agpat6	30520301	glycerol-3-phosphate acyltransferase 6 precursor
Alg2	172072657	alpha-1,3/1,6-mannosyltransferase ALG2
ATGL(Pnpla2)	254826780	patatin-like-phospholipase domain-containing protein 2 isoform 1
Ddhd2	254692989	phospholipase DDHD2
Dhrs1	31980844	dehydrogenase/reductase SDR family member 1
Dhrsx	124244062	dehydrogenase/reductase SDR family member on chromosome X homolog precursor
Faf2	158533976	FAS-associated factor 2
Gk5	28893497	putative glycerol kinase 5
Hsd17b7	87162470	3-keto-steroid reductase
Hsd17b11	16716597	estradiol 17-beta-dehydrogenase 11
Lss	22122469	lanosterol synthase
Lpcat1	148747363	lysophosphatidylcholine acyltransferase 1
Lpcat4	46402175	lysophospholipid acyltransferase LPCAT4
Nsdhl	31982437	sterol-4-alpha-carboxylate 3-dehydrogenase, decarboxylating
Pgs1	110626163	CDP-diacylglycerol – glycerol-3-phosphate 3-phosphatidyltransferase, mitochondrial
Rpn2	34996495	dolichyl-diphosphooligosaccharide – protein glycosyltransferase subunit 2 precursor
Lipid Droplet		
Abhd5	13385690	1-acylglycerol-3-phosphate O-acyltransferase ABHD5
Plin2	116235489	perilipin-2
Plin3	13385312	perilipin-3
Sccpdh	30520019	probable saccharopine dehydrogenase
Mitochondria		
Aco2	18079339	aconitate hydratase, mitochondrial precursor
Aifm2	30017355	apoptosis-inducing factor 2 isoform 2
Atp5a1	6680748	ATP synthase subunit alpha, mitochondrial precursor
Atp5b	31980648	ATP synthase subunit beta, mitochondrial precursor
Cyb5r3	19745150	NADH-cytochrome b5 reductase 3
Slc25a5	22094075	ADP/ATP translocase 2
Membrane Traffic		
Rab1	6679587	ras-related protein Rab-1A
Rab1	21313162	ras-related protein Rab-1B
Rab14	18390323	ras-related protein Rab-14
Rab18	30841008	ras-related protein Rab-18
Rab2a	10946940	ras-related protein Rab-2A
Vcp	225543319	transitional endoplasmic reticulum ATPase
Cytoskeleton		
Actn4	11230802	alpha-actinin-4
Acta2	6671507	actin, aortic smooth muscle

Canx	6671664	calnexin precursor
Gm5620	82930689	PREDICTED: tubulin alpha-1B chain isoform 4
Gm12715	309268166	PREDICTED: actin, cytoplasmic 2-like
Hist1h2bq	160420310	H2b histone family, member A
Hist1h4m	306482623	histone H4
H3f3a	94395561	histone H3.3-like isoform 1
Hist2h3c2	30089712	histone H3.2
Hist1h3a	21489955	histone H3.1
Hist2h2ab	119433657	histone H2A type 2-B
Nc1	84875537	nucleolin
Tuba1b	82930689	tubulin alpha-1B chain isoform 4
Tuba3a	6678465	tubulin alpha-3 chain
Tubb3	309265737	tubulin beta-3 chain-like
Tubb2a	33859488	tubulin beta-2A chain
Tubb5	7106439	tubulin beta-5 chain
Tubb6	27754056	tubulin beta-6 chain
Chaperone		
Dnaja1	6680297	dnaJ homolog subfamily A member 1
Hspa5	254540166	78 kDa glucose-regulated protein precursor
Hspa8	31981690	heat shock cognate 71 kDa protein
Hspa9	162461907	stress-70 protein, mitochondrial
Hsp90ab1	40556608	heat shock protein HSP 90-beta
Hsp90b1	6755863	endoplasmin precursor
Other Proteins		
Aup1	90403601	ancient ubiquitous protein 1
Cttn	309262863	src substrate cortactin
Ddx21	72384374	nucleolar RNA helicase 2
Ddx3x	6753620	ATP-dependent RNA helicase DDX3X
Eef1a1	126032329	elongation factor 1-alpha 1
Eef1a2	6681273	elongation factor 1-alpha 2
Eef2	33859482	elongation factor 2
Lmnb1	188219589	lamin-B1
Mettl7a2	61098178	methyltransferase like 7A2
Mybbp1a	31982724	myb-binding protein 1A
Nploc4	303324586	nuclear protein localization protein 4 homolog isoform A
Nus1	13384840	nogo-B receptor precursor
Pdia3	112293264	protein disulfide-isomerase A3 precursor
Tprgl	21312776	tumor protein p63-regulated gene 1-like protein
Top2a	153945749	DNA topoisomerase 2-alpha

studies (Wang *et al.*, 2015, Li *et al.*, 2016). The groups were as follows: Lipid Metabolism, Lipid Droplet, Mitochondria, Membrane Traffic, Cytoskeleton, Chaperone, and other proteins.

GO and KEGG pathway enrichment analyses of all proteins

To clarify the potential function of the proteins obtained in our experiment, GO and KEGG pathway enrichment analyses were performed. The GO enrichment

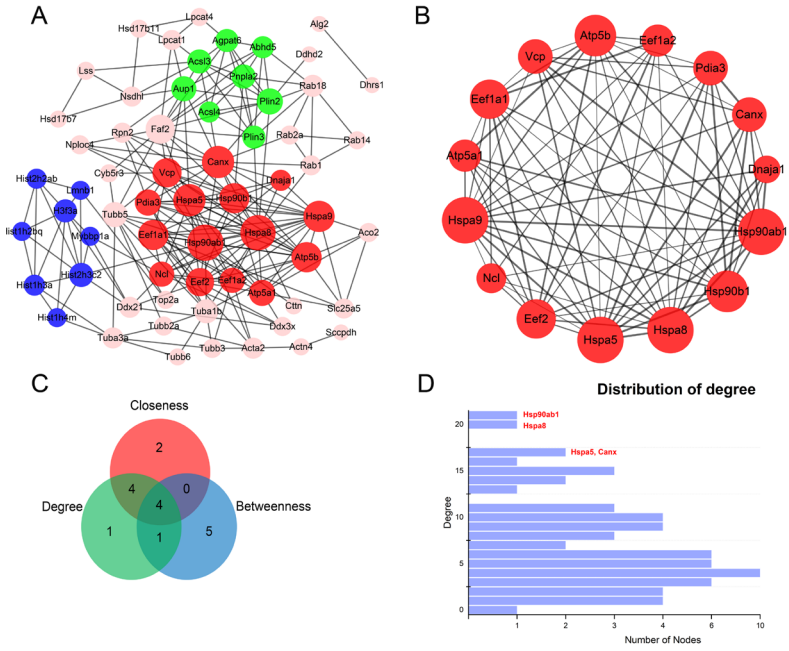

Figure 4. Protein-protein interaction (PPI) network and analyses of topological properties and modules.
(**A**) PPI network constructed by STRING using protein pairs with a combined score ≥ 0.4. Proteins were represented as nodes, with larger nodes representing proteins with more links. The edges represent the interactive relationships of proteins. The red, green, and blue nodes represent modules identified by MCODE. (**B**) Module with the highest significance (subnetwork_1). Larger nodes represent proteins with a higher degree, and thicker edges represent a higher combined score between two proteins. (**C**) Topological properties of the whole PPI network. Four proteins were simultaneously present in the lists of top 10 proteins with the highest degree, betweenness, and closeness. (**D**) The degree of distribution in the whole PPI network.

results showed that 127 GO terms were significantly enriched, including 78 BP terms, 19 CC terms, and 30 MF terms. KEGG enrichment analysis found that 10 pathways were significantly enriched. The top 10 most significantly enriched GO terms and KEGG pathways are shown in Supplementary Table 1 (at https://ojs.ptbioch.edu.pl/index.php/abp/). The GO terms that were most significantly enriched as BP, CC, and MF were endoplasmic reticulum to cytosol transport (GO: 0032482, *P*=3.91E-08), lipid droplet (GO:0005811, *P*=2.46E-22), and nucleoside binding (GO:0001882, *P*=1.03E-11), respectively. The most significantly enriched KEGG pathway was protein processing in the endoplasmic reticulum (KEGG:04141, *P*=5.75E-08). To illustrate the relationship between the terms and potential biological complexities, functionally grouped networks were constructed using the GO terms and KEGG pathways based on their shared genes. The proportion of each group, calculated from the number of terms, is displayed as pie charts. As shown in Fig. 2 and Fig. 3, the pathway containing the highest number of proteins was protein processing in the endoplasmic reticulum, which includes glycosylation of newly synthesized peptides and protein folding.

PPI network construction and module analysis

To identify the interactions between the proteins, a protein-protein interaction network (PPI) was constructed using the STRING V.11 database, with proteins having a combined score ≥0.4. As a result, 63 among 73 proteins were filtered into the PPI network, with 63 nodes and 230 edges. The MCODE algorithm was then applied, and three modules with highly correlated proteins were identified (Fig. 4A). The most significant module (sub-network1) included 15 nodes and 79 edges (Score=11.286, Fig. 4B). The topological properties of the whole PPI network were analyzed with regard to degree, betweenness, and closeness, which are three methods to measure the centrality of nodes, to understand the roles of specific proteins in the network (Fig. 4C). The top 10 proteins with the highest degree, betweenness, and closeness are listed in Supplementary Table 2 (at https://ojs.ptbioch.edu.pl/index.php/abp/). Four proteins, i.e. Hsp90ab1, Hspa8, Hspa5, and Canx, were present simultaneously in the lists of top 10 proteins with the highest degree, betweenness, and closeness. The degree distribution of the PPI network revealed that coincidently, these four proteins had the highest distribution degree (Fig. 4D). Meanwhile, the same proteins ap-

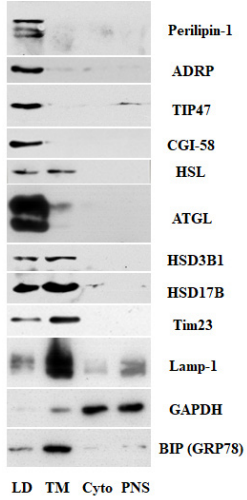

Figure 5. Confirmation of the identified LD proteins by immunoblotting.
Fractions of LDs, total membrane, cytosol, and post-nuclear supernatant were separated by SDS-PAGE and detected by immunoblotting.

peared in sub-network1 (Fig. 4B), which was the module with the highest score (Score=11.286) among the three modules identified. As the densely connected regions of the PPI network may represent molecular complexes and parts of pathways (Bader & Hogue, 2003), GO and KEGG enrichment analyses were performed for sub-network1 to further investigate its potential functions. GO enrichment analysis of the BP, CC, and MF found 16, 5, and 7 enriched terms, respectively, while the KEGG analysis revealed four enriched pathways; all enriched terms are listed in Supplementary Table 3 (at https://ojs.ptbioch.edu.pl/index.php/abp/). The most significant BP, CC, and MF terms were protein folding chaperone, myelin sheath, and unfolded protein binding, respectively, and the most enriched KEGG pathway was protein processing in the endoplasmic reticulum. Functionally grouped networks were also constructed to display the relationships between terms and proteins (Supplementary Fig. 1 (at https://ojs.ptbioch.edu.pl/index.php/abp/)).

Confirmation of the LD proteins identified in the N_2a cells by immunoblotting

To confirm the LD proteins identified, we tested the given proteins using the following protein markers, which corresponded to different cellular compartments. As shown in Fig. 5, Perilipin-1, ADRP, TIP147, CGI-58, HSL, ATGL, HSD3B1, HSD17B, Tim23, Lamp-1, and BIP (GRP78) proteins were detected in the LDs, but only Lamp-1 was detectable in the post-nuclear supernatant and cytosol compartments. In the TM compartments, we detected the HSL, ATGL, HSD3B1, HSD17B, Tim23, Lamp-1, and BIP (GRP78) proteins. This result confirmed that the isolated LD fraction of N_2a cells was free of contamination from other organelles.

DISCUSSION

LDs are involved in the normal physiological functions of the nervous system. In the work presented here, we report the proteomics of N_2a cell LDs for the first time. Seventy three proteins were purified and detected by HPLC-MS. Most proteins we discovered in the N2a cell LDs were also found in LDs of rat hearts and mouse testicular cells, as reported in previous studies (Wang *et al.*, 2015; Li *et al.*, 2016). However, some proteins of the N_2a cell LDs were also found in human hepatoma cell LDs (Sato *et al.*, 2006). We hypothesize that the different proteins found in different tissues may be species-related and tissue-related.

In our work, we detected the LD proteins related to membrane trafficking. The proteins were also involved in neuron function. For example, Rab18 is a critical regulator of morphogenesis and neuronal migration in the development of brains (Wu *et al.*, 2016). Rab1 plays an essential role in ER-to-Golgi trafficking, a key step in neuron formation. Moreover, Rab1 could help reduce the dopaminergic neuron loss induced by α-synuclein in a model of Parkinson's disease (PD) (Cooper *et al.*, 2006). These findings showed that LD proteins involved in membrane trafficking are related to neuronal functions.

Hsp90ab1, Hspa8, and Hspa5 are proteins from the HSP90 and HSP70 families; they are conserved ATP-dependent molecular chaperones that fold and remodel proteins. However, HSP90 might also be a contaminant in this work. These proteins are important components of the cellular machinery involved in protein homeostasis, and they participate in nearly every cellular process (Genest *et al.*, 2019). Calnexin, a type of chaperone, interacts with many nascent membrane and soluble proteins of the secretory pathway; one of its demonstrated functions is eliminating incorrectly or incompletely folded proteins (Bergeron *et al.*, 1994). These findings may partly explain the extensive interactions of these four proteins with others. Biological process enrichment indicated that Hspa5, Hspa8, Hspa9, and Dnaja1 are involved in protein folding and refolding as molecular chaperones. Hspa5, Vcp, and Hsp90b1 are included in the endoplasmic-reticulum-associated protein degradation pathway, which targets endoplasmic reticulum-resident proteins for degradation by the cytoplasmic proteasome.

Intracellular lipids are stored in LDs and metabolized to supply lipids for the cell. ALG2, which was found in the LDs, participates in the lipid-linked oligosaccharide synthesis related to AD through ceramide and cholesterol metabolism (Cutler *et al.*, 2004). Robust evidence suggests that the alteration of lipid metabolism could play an important role in neurodegeneration (Yadav & Tiwari, 2014). In previous studies, high plasma cholesterol levels were found to be a risk factor for AD (Tan *et al.*, 2003). Besides, the plasma lipid and lipoprotein levels are related to AD (Romas *et al.*, 1999). Several studies have also concluded that lipids are an important modifier of α-synuclein toxicity, contributing to PD (Xu & Huang, 2006). Meanwhile, increasing evidence suggests that altered lipid metabolism could be a general mechanism underlying neurodegeneration. Our findings showed that LDs might be involved in the pathogenesis of neurodegenerative diseases.

Brain function depends on coordinated interactions between neurons and glial cells (Perea *et al.*, 2014). Neurons and glia in the CNS have been reported to secrete exosomes into the extracellular environment (Vaccari *et al.*, 2016). Exosome secretion has two general functions: signaling to neighboring cells by horizontal transfer of biomolecules and disposal of unnecessary cell components (Fruhbeis *et al.*, 2012b). There are many proteins involved in this process, such as the cytoskeleton–tubulin protein and chaperone protein HSP90 (Fruhbeis *et al.*, 2012a, Terni *et al.*, 2017). We also detected these proteins in LDs, showing that LDs are associated with exosome secretion in the nervous system.

Through the proteomics analysis of N_2a cell LDs, we also found several proteins that were not a part of any group. These proteins were also involved in neuronal function and nervous system diseases. For example, we detected Pdia3 and eEF1A2 in LDs. Pdia3 is a multifunctional protein hypothesized to be a membrane receptor for 1,25(OH)2D3, which is involved in neuroprotection *in vitro* (Pendyala *et al.*, 2012, Zhang *et al.*, 2015). Translation-elongation factor eEF1A2 was only detected in the N_2a cell LDs. However, eEF1A2 might also be a contaminant in this work. In a previous study, eEF1A2 was found to be related to neuron degeneration, and it was present only in the brain (Newbery *et al.*, 2007). The loss of activity of eEF1A2 in mice was associated with vacuolar degeneration in motor neurons; therefore, eEF1A2 may be involved in neurodegenerative diseases.

Cellular component enrichment analysis revealed that most proteins of the sub-network were located in the myelin sheath. Molecular function enrichment showed that several proteins participated in unfolded protein-binding and translation-elongation factor activity, similar to the case of biological process enrichment analysis. It is noteworthy that Atp5a1, Atp5b, and Vcp were involved in major histocompatibility complex (MHC)-class I protein binding; these are a set of molecules displayed

on cell surfaces responsible for lymphocyte recognition and antigen presentation, which are related to immunity in the CNS. KEGG pathways were enriched in protein processing in the endoplasmic reticulum, antigen processing and presentation, thyroid hormone synthesis, and legionellosis. Thus, LDs might be involved in the normal physiology and pathophysiology of the central nervous system. However, due to the limitations of the in *vitro* model, further research is required to clarify the functions of LD proteins in *vivo*.

CONCLUSION

In summary, for the first time, we conducted the proteomics analysis of LDs in the N_2a cells. We found that in N_2a cells, LDs are distributed in the whole cytoplasm. By HPLC-MS, we detected 73 proteins in the N_2a cells that are mostly involved in the normal physiological functions and the pathophysiology of the nervous system. Our results may provide a clearer understanding of the role of LDs in the nervous system, providing new insights regarding their role in neurodegenerative diseases.

Conflict of Interest

The authors declare that the research was conducted in the absence of any commercial or financial relationships that could be construed as a potential conflict of interest.

Availability of data and materials

All data generated or analyzed during this study are included in this published article.

Authors' contributions

Weiyi Wang and Hecheng Wang designed and supervised the study. Weiyi Wang, Jiahao Guan, Yu Zong, Qiuxian Zhang analyzed the data, interpreted the data, Wei Zhang and Hecheng Wang prepared the manuscript for publication and reviewed the draft of the manuscript. All authors have read and approved the manuscript.

REFERENCE

Amazzal L, Lapotre A, Quignon FBagrel D (2007) Mangiferin protects against 1-methyl-4-phenylpyridinium toxicity mediated by oxidative stress in N2A cells. *Neurosci Lett.* **418**: 159–164. https://doi.org/10.1016/j.neulet.2007.03.025

Ashburner M, Ball CA, Blake JA, Botstein D, Butler H, Cherry JM, Davis AP, Dolinski K, Dwight SS, Eppig JT, Harris MA, Hill DP, Issel-Tarver L, Kasarskis A, Lewis S, Matese JC, Richardson JE, Ringwald M, Rubin GMSherlock G (2000) Gene ontology: tool for the unification of biology. The Gene Ontology Consortium. *Nat Genet* **25**: 25–29. https://doi.org/10.1038/75556

Bader GDHogue CW (2003) An automated method for finding molecular complexes in large protein interaction networks. *BMC Bioinformatics* **4**: 2. https://doi.org/10.1186/1471-2105-4-2

Bergeron JJ, Brenner MB, Thomas DYWilliams DB (1994) Calnexin: a membrane-bound chaperone of the endoplasmic reticulum. *Trends Biochem Sci* **19**: 124–128. https://doi.org/10.1016/0968-0004(94)90205-4

Bindea G, Mlecnik B, Hackl H, Charoentong P, Tosolini M, Kirilovsky A, Fridman WH, Pages F, Trajanoski ZGalon J (2009) ClueGO: a Cytoscape plug-in to decipher functionally grouped gene ontology and pathway annotation networks. *Bioinformatics* **25**: 1091–1093. https://doi.org/10.1093/bioinformatics/btp101

Cooper AA, Gitler AD, Cashikar A, Haynes CM, Hill KJ, Bhullar B, Liu K, Xu K, Strathearn KE, Liu F, Cao S, Caldwell KA, Caldwell GA, Marsischky G, Kolodner RD, Labaer J, Rochet JC, Bonini NMLindquist S (2006) Alpha-synuclein blocks ER-Golgi traffic and Rab1 rescues neuron loss in Parkinson's models. *Science* **313**: 324–328. https://doi.org/10.1126/science.1129462

Cutler RG, Kelly J, Storie K, Pedersen WA, Tammara A, Hatanpaa K, Troncoso JCMattson MP (2004) Involvement of oxidative stress-induced abnormalities in ceramide and cholesterol metabolism in brain aging and Alzheimer's disease. *Proc Natl Acad Sci U S A* **101**: 2070–2075. https://doi.org/10.1073/pnas.0305799101

Fruhbeis C, Frohlich DKramer-Albers EM (2012a) Emerging roles of exosomes in neuron-glia communication. *Front Physiol* **3**: 119. https://doi.org/10.3389/fphys.2012.00119

Fruhbeis C, Frohlich DKramer-Albers EM (2012b) Emerging roles of exosomes in neuron-glia communication. *Frontiers Physiol* **3**. https://doi.org/10.3389/fphys.2012.00119

Fuller MFuterman AH (2018) The brain lipidome in neurodegenerative lysosomal storage disorders. *Biochem Biophys Res Commun* **504**: 623–628. https://doi.org/10.1016/j.bbrc.2018.03.042

Genest O, Wickner SDoyle SM (2019) Hsp90 and Hsp70 chaperones: Collaborators in protein remodeling. *J Biol Chem* **294**: 2109–2120. https://doi.org/10.1074/jbc.REV118.002806

Kory N, Farese RV, Jr.Walther TC (2016) Targeting Fat: Mechanisms of Protein Localization to Lipid Droplets. *Trends Cell Biol* **26**: 535–546. https://doi.org/10.1016/j.tcb.2016.02.007

Li L, Zhang H, Wang W, Hong Y, Wang J, Zhang S, Xu S, Shu Q, Li J, Yang F, Zheng M, Qian ZLiu P (2016) Comparative proteomics reveals abnormal binding of ATGL and dysferlin on lipid droplets from pressure overload-induced dysfunctional rat hearts. *Sci Rep* **6**: 19782. https://doi.org/10.1038/srep19782

Liu L, Zhang K, Sandoval H, Yamamoto S, Jaiswal M, Sanz E, Li Z, Hui J, Graham BH, Quintana ABellen HJ (2015) Glial lipid droplets and ROS induced by mitochondrial defects promote neurodegeneration. *Cell* **160**: 177–190. https://doi.org/10.1016/j.cell.2014.12.019

Murphy DJ (2012) The dynamic roles of intracellular lipid droplets: from archaea to mammals. *Protoplasma* **249**: 541–585. https://doi.org/10.1007/s00709-011-0329-7

Newbery HJ, Loh DH, O'Donoghue JE, Tomlinson VA, Chau YY, Boyd JA, Bergmann JH, Brownstein DAbbott CM (2007) Translation elongation factor eEF1A2 is essential for post-weaning survival in mice. *J Biol Chem* **282**: 28951–28959. https://doi.org/10.1074/jbc.M703962200

Pendyala G, Ninemire CFox HS (2012) Protective role for the disulfide isomerase PDIA3 in methamphetamine neurotoxicity. *PLoS One* **7**: e38909. https://doi.org/10.1371/journal.pone.0038909

Perea G, Sur MAraque A (2014) Neuron-glia networks: integral gear of brain function. *Front Cell Neurosci* **8**: 378. https://doi.org/10.3389/fncel.2014.00378

Romas SN, Tang MX, Berglund LMayeux R (1999) APOE genotype, plasma lipids lipoproteins, and AD in community elderly. *Neurology* **53**: 517–521. https://doi.org/10.1212/wnl.53.3.517

Sachana M, Flaskos J, Alexaki EHargreaves AJ (2003) Inhibition of neurite outgrowth in N2a cells by leptophos and carbaryl: effects on neurofilament heavy chain, GAP-43 and HSP-70. *Toxicol In Vitro.* **17**: 115–120. https://doi.org/10.1016/s0887-2333(02)00121-2

Sato S, Fukasawa M, Yamakawa Y, Natsume T, Suzuki T, Shoji I, Aizaki H, Miyamura TNishijima M (2006) Proteomic profiling of lipid droplet proteins in hepatoma cell lines expressing hepatitis C virus core protein. *J Biochem* **139**: 921–930. https://doi.org/10.1093/jb/mvj104

Shannon P, Markiel A, Ozier O, Baliga NS, Wang JT, Ramage D, Amin N, Schwikowski BIdeker T (2003) Cytoscape: a software environment for integrated models of biomolecular interaction networks. *Genome Res* **13**: 2498–2504. https://doi.org/10.1101/gr.1239303

Szklarczyk D, Gable AL, Lyon D, Junge A, Wyder S, Huerta-Cepas J, Simonovic M, Doncheva NT, Morris JH, Bork P, Jensen LJMering CV (2019) STRING v11: protein-protein association networks with increased coverage, supporting functional discovery in genome-wide experimental datasets. *Nucleic Acids Res* **47**: D607–D613. https://doi.org/10.1093/nar/gky1131

Tan ZS, Seshadri S, Beiser A, Wilson PWF, Kiel DP, Tocco M, D'Agostino RBWolf PA (2003) Plasma total cholesterol level as a risk factor for Alzheimer disease – The Framingham study. *Archives Int Med* **163**: 1053. https://doi.org/10.1001/archinte.163.9.1053

Terni B, Lopez-Murcia FJLlobet A (2017) Role of neuron-glia interactions in developmental synapse elimination. *Brain Res Bull* **129**: 74–81. https://doi.org/10.1016/j.brainresbull.2016.08.017

The Gene Ontology C (2019) The Gene Ontology Resource: 20 years and still GOing strong. *Nucleic Acids Res* **47**: D330–D338. https://doi.org/10.1093/nar/gky1055

Tremblay RG, Sikorska M, Sandhu JK, Lanthier P, Ribecco-Lutkiewicz MBani-Yaghoub M (2010) Differentiation of mouse Neuro 2A cells into dopamine neurons. *J Neurosci Methods* **186**: 60–67. https://doi.org/10.1016/j.jneumeth.2009.11.004

Vaccari JPD, Brand F, Adamczak S, Lee SW, Perez-Barcena J, Wang MY, Bullock MR, Dietrich WDKeane RW (2016) Exosome-mediated inflammasome signaling after central nervous system injury. *J Neurochem* **136**: 39–48. https://doi.org/10.1111/jnc.13036

Wang W, Wei S, Li L, Su X, Du C, Li F, Geng B, Liu PXu G (2015) Proteomic analysis of murine testes lipid droplets. *Sci Rep* **5**: 12070. https://doi.org/10.1038/srep12070

Welte MA (2015) How brain fat conquers stress. *Cell.* **163**: 269–270. https://doi.org/10.1016/j.cell.2015.09.046

Westergard T, Jensen BK, Wen X, Cai J, Kropf E, Iacovitti L, Pasinelli PTrotti D (2016) Cell-to-Cell transmission of dipeptide repeat proteins linked to C9orf72-ALS/FTD. *Cell Rep.* **17**: 645–652. https://doi.org/10.1016/j.celrep.2016.09.032

Wichmann H, Vocke F, Brinkhoff T, Simon MRichter-Landsberg C (2015) Cytotoxic effects of tropodithietic acid on mammalian clonal cell lines of neuronal and glial origin. *Mar Drugs* **13**: 7113–7123. https://doi.org/10.3390/md13127058

Wu Q, Sun X, Yue W, Lu T, Ruan Y, Chen TZhang D (2016) RAB18, a protein associated with Warburg Micro syndrome, controls neuronal migration in the developing cerebral cortex. *Mol Brain* **9**: 19. https://doi.org/10.1186/s13041-016-0198-2

Xu QHuang YD (2006) Lipid metabolism in Alzheimer's and Parkinson's disease. *Future Lipidology* **1**: 441–453. https://doi.org/10.2217/17460875.1.4.441

Yadav RSTiwari NK (2014) Lipid integration in neurodegeneration: an overview of Alzheimer's disease. *Mol Neurobiol* **50**: 168–176. https://doi.org/10.1007/s12035-014-8661-5

Yu JH, Zhang SY, Cui LJ, Wang WY, Na HM, Zhu XT, Li LH, Xu GH, Yang FQ, Christian MLiu PS (2015) Lipid droplet remodeling and interaction with mitochondria in mouse brown adipose tissue during cold treatment. *Biochim Biophys Acta – Mol Cell Res* **1853**: 918–928. https://doi.org/10.1016/j.bbamcr.2015.01.020

Zhang CLiu P (2017) The lipid droplet: A conserved cellular organelle. *Protein Cell* **8**: 796–800. https://doi.org/10.1007/s13238-017-0467-6

Zhang XQ, Pan Y, Yu CH, Xu CF, Xu L, Li YMChen WX (2015) PDIA3 Knockdown exacerbates free fatty acid-induced hepatocyte steatosis and apoptosis. *PLoS One* **10**: e0133882. https://doi.org/10.1371/journal.pone.0133882